Original Article

Analytical evaluation of the peak contact pressure in a rectangular elastomeric seal with rounded edges

Antonio Strozzi, Enrico Bertocchi, Sara Mantovani, Matteo Giacopini and Andrea Baldini

Department of Engineering "Enzo Ferrari", University of Modena and Reggio Emilia, Modena, Italy

Corresponding author:

Enrico Bertocchi, Department of Engineering "Enzo Ferrari", University of Modena and Reggio Emilia, Via Vivarelli 20, 41125 Modena, Italy.

Email: ebertocchi@unimore.it

Abstract

The contact pressure is considered for an elastomeric rectangular seal with rounded edges. An asymptotic matching is performed between an available analytical expression of the contact pressure that neglects the finiteness of the seal dimensions, and a fracture mechanics solution describing a periodically laterally cracked strip of finite width. This matching provides a corrected formula for the peak contact pressure that accounts for the finiteness of the seal dimensions. The analytical expression for the peak contact pressure is validated versus Finite Element (FE) predictions for a large family of seal

geometries and, in particular, for a seal reference shape extracted from the pertinent literature. An appraisal of the finite deformation effect has been carried out numerically.

Keywords

Elastomeric seal, contact pressure, asymptotic matching, fracture mechanics, Finite Elements.

Introduction

Rectangular elastomeric seals, *e.g.* Nikas et al.[1] constitute an alternative design to O-rings, *e.g.* George et al.[2] Figure 1 displays a rectangular seal with rounded edges, and it clarifies the meaning of the main symbols adopted, namely the seal width, *w*, its height, *h*, the rounded edge radius, *r*, and the extent, *a*, of the material laterally protruding beyond the flat portion of the sealing profile.

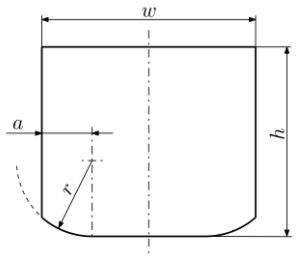

Figure 1. The shape of the rectangular seal, and the definition of the main symbols adopted.

Rectangular seals are employed in demanding applications such as aircraft actuators, *e.g.* Ruskell.[3] They are also commonly used as gaskets in gear pumps; their shape

follows the geometry of the flange/cover border, and, therefore, they are moulded on purpose.

The edges of rectangular seals for reciprocating motion may be manufactured as square, see Ruskell.[3] In this case, wear produces chamfers at the extremities of the contact profile, whose shape and size are somewhat indeterminate. Alternatively, the seal edges are manufactured as rounded, see Strozzi.[4]

As a consequence of the presence of rounded edges, the contact pressure exhibits Hertzian-type local bumps in its lateral zones; it remains almost flat in the central zone of the contact; it becomes null at the contact extremities. The lateral bumps and the central flattish zone confer to the contact pressure distribution a camel-backed profile, see Strozzi,[4] and Strozzi et al.,[5] for a similar axisymmetric problem.

An analysis of the properties of specific seal profiles is more relevant when the profile is not appreciably altered by wear, hence in static applications and in low-cycle dynamic employments.

The stress field within an elastomeric seal and, in particular, its contact pressure distribution, are useful indicators of the seal performance both in static and in elasto-hydrodynamic lubrication regimes; the evaluation of the peak contact pressure constitutes the primary scope of this paper.

In Strozzi,[4] an approximate model is proposed to compute the contact pressure profile, based upon a fictitious segmentation of the rectangular seal into simple

substructures. It is however difficult to derive a more rigorous analytical expression of the contact pressure curve for the title problem. In fact, the analytical solution available for a rectangular punch with rounded edges, pressed against a half plane, *e.g.* Ciavarella et al.,[6] and related bibliography, is exact only in the situation of a rigid punch indenting a deformable half plane, see Strozzi et al.,[7] whereas in the title problem the punch (*i.e.* the seal) is flexible and the half plane (*i.e.* the counterface) is rigid. In fact, the analytical solution of Ciavarella et al.[6] relies on the Boussinesq foundation model, which, holding for an infinite half plane, cannot account for the effect of the seal finite width and height.

It has recently been shown in Strozzi et al.,[7] Sackfield et al.,[8] and Banerjee et al.,[9] that the unrealities of the above analytical solution may be corrected, and the finiteness of the indenter dimensions may be accounted for, by combining the above analytical solution with Fracture Mechanics (FM) results dealing with the stress singularities at the tip of a transverse crack in a strip of finite width. This combination relies on a matching between two asymptotic solutions, namely a) the analytical pressure profile valid for a frictionless, plane, rounded rigid indenter of semi-infinite width, and b) the corresponding pressure profile describing the sharp-edged equivalent of the problem under scrutiny. The sharp-edged equivalent problem is modelled in terms of FM, where the crack length coincides with the width of the indenter material projecting beyond the contact extremities; for the commonplace situation of indenter

rounded edges described by a quarter circumference and for moderate compressions, the projection width may be assumed to coincide with the edge radius, see Figure 1.

Equation (20) for the peak contact pressure obtained in Strozzi et al.,[7] has been developed for a deformable rectangular punch with rounded edges and of infinite width and height; in addition, it is assumed that the seal rounded edges are described by a quarter circumference; the preliminary assessments of this formula, presented in Strozzi et al.,[7] have indicated that this approach is accurate in modelling a deformable punch compressed against a rigid half plane. However, in the seal realm the rounded portion may be less than a quarter of circumference, see Figure 1 of Strozzi,[4] and Prati and Strozzi.[10]

This paper aims at developing an extension of formula (20) of Strozzi et al,[7] that accounts for the combined effects of a) finite seal width and height, and b) a rounded corner described by an incomplete quarter circumference. This improved formula has been achieved by asymptotically matching i) the Boussinesq solution of Sackfield et al.,[8] for a frictionless rigid indenter of semi-infinite width whose edge is rounded, with ii) a stress intensity factor derived from the FM realm, describing a strip under tension, exhibiting lateral transverse periodic collinear cracks. An extensive error analysis of the formula proposed for the evaluation of the peak contact pressure is diagrammatically presented.

The paper is organized as follows. A literature review highlights the specific problems encountered in the design of rectangular elastomeric seals. The peak contact pressure for a semi infinite rigid punch with rounded edges indenting a deformable half plane, and a FM solution expressing the stress singularities at the tips of transverse cracks in a strip of finite width are presented in specific sections. A formulation is then derived, that estimates the mean stress encountered in the FM solution in terms of the strip deformation, which corresponds to the seal fractional compression; this compression is the most relevant design parameter in practical applications. The two solutions are then asymptotically matched to derive an analytical expression for the peak contact pressure in terms of the seal fractional compression, that accounts for the seal finite width and height. Addressing a representative seal geometry extracted from the pertinent bibliography, Strozzi[4], a specific numerical evaluation is presented of the robustness of the asymptotic matching formula as the extent of the contact beyond the initial region becomes finite (as opposed to infinitesimal), a condition, this, typical of elastomeric seals. Then, an extensive FE campaign is carried out on a family of rectangular seal cross sections to quantify the error of the above design formulae, inside the small deformation assumptions, and an illustrative comparison with a case extracted from literature is included. Finally, an extension of the FE campaign to the large deformation realm is presented, and a comparison with a literature case is included.

Literature review

This bibliographic survey addresses several aspects, namely the geometry of the rectangular seal (and its fractional compression), the shape of the seal contact pressure profile, the influence on the pressure profile of the sealed pressure, the effect of large deformations, the sensitivity of the contact pressure profile to perturbations of the Poisson's ratio, and the relevance of the stress-strain law adopted.

The rectangular seal edges may be manufactured as square, see Ruskell.[3] In this case, wear produces chamfers whose shape and size are indeterminate. The SAEJ120R2 standards address rectangular section rubber seal rings for automotive applications, but the main interest is focused on the groove geometry rather than on details of the seal cross section. In Figure 6 of the recent paper by Nikas et al.,[1] dealing with rectangular seals, the dimensions describing a break edge are provided for the seal edges at the extremities of the sealing profile, thus seemingly indicating that, from a technical viewpoint, rounded or chamfered edges are indifferently employed.

Indications extracted from the pertinent literature on the rectangular seal geometries of technical interest, Figure 1, are as follows. The ratio r/w , where r is the radius of the seal rounded edge and w is the seal width, ranges from 0.0125 to 0.265, see Strozzi,[4] Prati and Strozzi,[10] Nikas and coworkers,[11-17] Stupkiewicz and Marciniszyn[18]. The ratio w/h, where w is the seal width and h is the seal height, ranges between 0.8 and 1.13, see Strozzi,[4] Prati and Strozzi,[10] Nikas and Sayles.[15] Often the radiused corners are

described by a quarter circle; however, applications are known in which the seal rounded corners are described by a portion of a quarter of circumference, see Strozzi,[4] and Prati and Strozzi.[10]

Moving to the shape of the seal contact pressure profile, as a result of the presence of rounded seal edges, the seal contact pressure exhibits two lateral pressure bumps, whereas the contact pressure remains flattish in the contact central zone. On the whole, the contact profile is camel-backed, see Strozzi,[4] Strozzi et al.,[5,7] Prati and Strozzi,[10] Medri and Strozzi,[19] Rana et al.,[20] and Stupkiewicz and Marciniszyn.[18]

Apparently, the presence of lateral pressure bumps promoted by the rounded edges was first noticed in Dowson and Swales.[21] In Field and Nau,[22-24] limited lateral pressure bumps were found. In Field and Nau,[22] it was commented that "the reason why the pressure peaks are absent in the present work is not clear".

The influence on the pressure profile of the sealed pressure is examined below. The presence of a sealed pressure modifies the dry contact pressure distribution evaluated in its absence. In Lindley,[25] the effect of a pressure difference across an O-ring seal is considered with particular regard to the possible occurring of leakage.

Moving to rectangular seals, in Ruskell,[3] the dry contact pressure distribution in the presence of a sealed pressure is estimated by adding the sealed pressure to the contact pressure distribution evaluated in the absence of sealed pressure. The numerical forecasts presented in Figure 9 of Stupkiewicz and Marciniszyn[18] agree with this

assumption. However, the experimental results of Field and Nau[22] show that in some cases the central flat portion of the contact pressure remains essentially horizontal, whereas in other situations it perceivably tilts as a result of the combined effect of the sealed pressure and of the frictional forces, see Prati and Strozzi,[10] and Stupnicki[26]. As an alternative method to that favoured in Ruskell,[3] in Prati and Strozzi[10] it has been proposed to estimate the contact pressure distribution in the presence of a sealed pressure by adding to the contact pressure, evaluated in the absence of a sealed pressure, a linear distribution, whose values at the seal edges are the sealed and the atmospheric pressure, respectively. Since the main aim of this paper is to evaluate the peak contract pressure, the two above described models, that is, the model ignoring the pressure tilting, and the model mimicking a pressure tilting, concur in favouring the practical rule of thumb according to which the peak contact pressure may be estimated as the sum of a) the lateral pressure bump computed in the absence of a sealed pressure, and b) the sealed pressure.

The effect of large deformations is discussed below. Although the seal compressions may reach values as high as 20 per cent, in the interest of simplicity linear elasticity is generally employed in the literature, especially in the analytical studies. Some information on the effect of large deformations may be extracted from Dragoni and Strozzi,[27] where the mismatch between the solutions in small and large

deformations was found to be of the order of the fractional compression imposed, see also Strozzi and Unsworth[28].

The sensitivity of the stress field to perturbations of the Poisson's ratio (or, equivalently, of the bulk modulus) of the elastomeric material is examined in the following. For elastomeric materials, the Poisson's ratio, which quantifies the cubic compressibility of the elastomer, is very close to the ideal incompressibility value 0.5; this threshold is often adopted in the mechanical analysis of elastomeric units, see Lindley,[29] and Allen et al.,[30] since its exact value is difficult to measure, see Strozzi.[31]

Well documented cases are available in which the stress field of the elastomeric unit highly depends on the cubic compressibility of the material, especially when the elastomeric component is bonded to a rigid surface, *e.g.* Holownia.[32] Encouragingly, it was numerically found in Prati and Strozzi,[10] that for a rectangular seal the contact pressure is essentially independent of the cubic compressibility adopted for the elastomeric material, provided that the Poisson's ratio is higher than, say, 0.489. The limited influence of the Poisson's ratio for the title geometry may be rationalized by observing that the seal border is not bonded to a rigid counterface, see also Strozzi and Unsworth.[28]

The importance of the constitutive relation (*i.e.* the stress-strain law) for elastomeric materials is considered hereinafter. The nonlinear stress-strain response in elastomeric materials subjected to large deformations is generally expressed by a strain

energy function formulated in terms of the three Rivlin strain invariants. The sensitivity of the seal stress field to the formulation of the strain energy function has been numerically assessed in Prati and Strozzi[10] and in Nikas and Sayles,[14-15] for a rectangular seal by comparing an experimentally calibrated expression of the strain energy function, see Medri and Strozzi,[33] to a compressible neo-Hookean law, the Young's modulus for infinitesimal strains being the same for the two cases. A discrepancy lower than 10 per cent is perceivable in the vicinity of the pressure bumps, where the deformations are highest, see also Nikas and Sayles.[14-15]

Simplifying assumptions

The simplifying assumptions adopted are justified by the indications retrieved from the literature survey. Linear elasticity in plane strain is adopted, and a reference value is attributed to the Poisson's ratio, namely $\nu = 0.489$. The contact between the seal and the counterface is assumed as frictionless. The contact pressure profile is evaluated in the absence of a sealed pressure. Only for the section entitled *"Numerical assessment of the error incurred by large deformations"*, large deformations have been used in conjunction with a neo-Hookean constitutive law.

Design formula for the contact pressure peak

In this section, an analytical expression of the peak contact pressure for a rectangular seal with rounded edges, compressed against a rigid counter plane, is obtained by combining the analytical solution available for a rigid rectangular punch with rounded edges and of semi-infinite width indenting a deformable half plane of Strozzi et al.,[7] Sackfield et al.,[8] and Banerjee et al.,[9] with a FM solution dealing with the stress singularities at the tips of transverse cracks in a strip of finite width. This combination is expected to correct the unrealities of the above analytical solution, and to account for the finiteness of the indenter dimensions. The above combination relies on a matching between the two above mentioned asymptotic solutions, detailed in the two following Sections.

The analytical contact pressure profile for an indenter of semi-infinite width

The analytical contact pressure p for a plane, frictionless, rounded, rigid punch of semi-infinite width, compressed against a deformable half plane, see Sackfield et al.,[8] is:

$$p(\xi) = \frac{E^*}{2\pi r}\left[2\sqrt{\xi d} + \xi - d\log\left(\frac{\sqrt{d}-\sqrt{\xi}}{\sqrt{d}+\sqrt{\xi}}\right)\right] \tag{1}$$

in which the ξ coordinate spans the contact length starting from the contact extremity. In addition, d denotes the unknown extent of the contact along the radiused region, r is the

radius of the rounded edge, and E^* is the equivalent Young's modulus. It is recalled that the above expression relies on the Boussinesq foundation model, which, holding for an infinite half plane, cannot account for the effect of the finite punch width and height.

The above expression (1) has been obtained in Sackfield et al.,[8] by performing a limit of the solution of Ciavarella et al.,[6] referring to an indenter of finite width. In Strozzi et al.,[7] the same formula has been obtained by directly referring to an indenter of semi-infinite width.

The maximum contact pressure $p_{\max}$ according to expression (1), see Strozzi et al.,[7] and Sackfield et al.,[8] is:

$$\frac{p_{\max}}{E^*} \cong 0.382\ \frac{d}{r} \tag{2}$$

In addition, for large ξ values, the contact pressure (1) asymptotically varies with ξ as, Sackfield et al.,[8]

$$p(\xi) \approx \frac{2E^*\sqrt{d^3}}{3\pi r}\frac{1}{\sqrt{\xi}}, \quad \xi >> d, \xi << a, w, h \tag{3}$$

where a, w, and h are the characteristic dimensions of the problem, described in Figure 1.

FM expression derived from existing solutions

It has already been mentioned that, following Sackfield et al.,[8] the unrealities of the analytical solution may be corrected by matching two asymptotic solutions, namely a) the analytical pressure profile valid for a frictionless, plane, rounded rigid punch of semi-infinite width indenting a deformable half-plane, and b) the corresponding pressure profile describing a FM equivalent of the problem under scrutiny.

Figure 2a illustrates on the left the basic seal cross section, rounded along the lower border and whose upper profile is flat, of height *h*. It also includes on the right a variant of doubled height in which the upper border is equally rounded, which may be reconducted to the basic geometry.

The FM equivalent should account for three main aspects of the seal deformation. First, it should consider the effect of the seal material protruding from the contact region. Secondly, it should account for two parts of the rectangular seal border remaining rectilinear under compression, namely a) the flat portion of the sealing profile, and b) the seal opposite flat side. Third, the FM problem should account for the interaction between the two lateral pressure peaks, when the seal flat portion is limited.

These three properties may be mimicked by a FM solution dealing with a laterally cracked strip of finite width, and by imposing that the strip exhibits, in addition to its vertical axis, two transverse symmetry axes, the first axis passing through two collinear edge cracks, and the second axis being parallel to the previous one and at a

distance equal to the seal height. A suitable FM model is therefore an infinitely long strip of finite width under remote tension σ, exhibiting an infinite array of equispaced, transverse, collinear edge cracks, see Figure 2b, in which the above symmetry axes are evidenced.

It is noted that, since in practice the seal is compressed, whilst the cracked strip is elongated, the sign convention for the two nominal stresses is opposite.

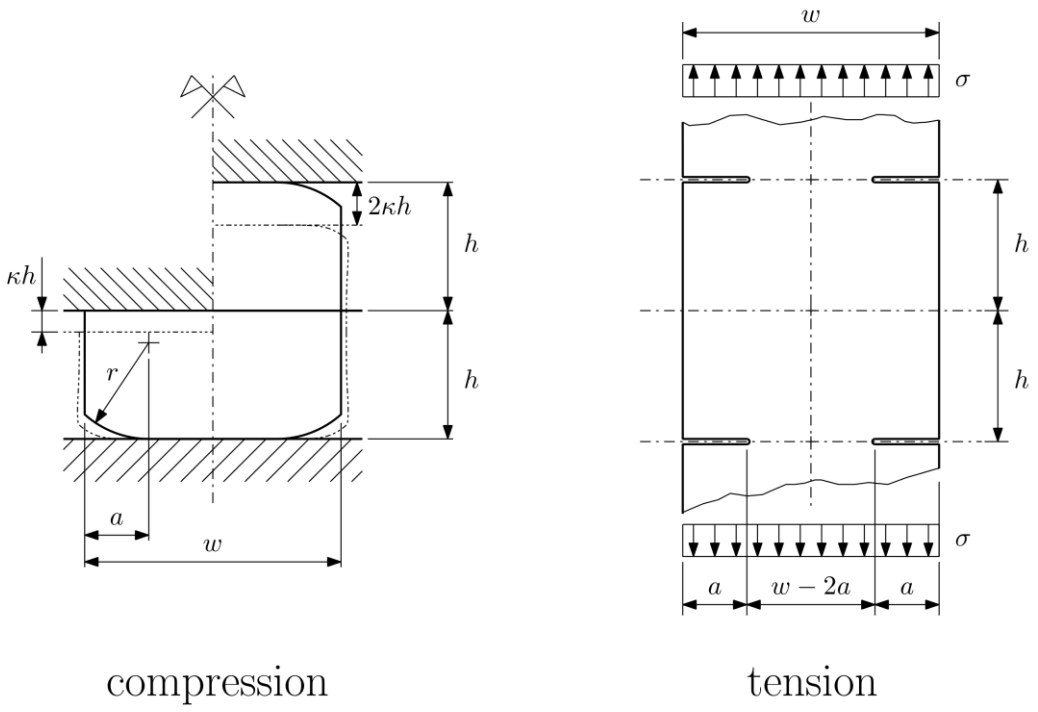

(a) (b)

Figure 2. The seal geometry (a) in its undeformed (solid line) and compressed (dotted line) configuration, compared with the proposed FM model (b), in the undeformed configuration under traction.

By assuming that the contact extent of the seal rounded profile is sufficiently small, the crack width, *a*, coincides with the width of the rounded portion of the seal profile. The equivalence between the seal cross section and the crack strip also requires that the distance between two parallel contiguous cracks is equal to twice the seal height, *h*, and that *w* is both the seal finite width and the strip width, see Figure 2.

A parametric solution to the above FM problem does not appear to be traceable in the pertinent literature; the most similar available problems are probably a) two collinear transverse edge cracks in a strip of finite width, for which an interpolating formula is reported in Tada et al.,[34] p. 46; b) an infinite array of periodic, parallel, edge cracks in a semi-infinite plane, for which an analytical expression is supplied in Tada et al.,[34] p. 264, only for very large or very small values of the period, whereas, for intermediate values of the period, a graphical representation is provided; c) an infinite array of transverse, central (as opposed to edge) cracks in a strip of finite width, for which only a graphical representation is presented in Tada et al.,[34] p. 285.

In the following, a formula for the above FM problem is proposed that is derived by combining the aforementioned cases a) and b). In fact, for the case a) the (rearranged) expression of K_I is:

$$K_I = 1.122 \frac{f\left(\frac{2a}{w}\right)}{\sqrt{1-\frac{2a}{w}}} \sigma \sqrt{\pi a} \tag{4}$$

where the expression of f is:

$$f\left(\frac{2a}{w}\right) = 1.000 - 0.500 \frac{2a}{w} - 0.183 \left(\frac{2a}{w}\right)^2 + 0.420 \left(\frac{2a}{w}\right)^3 - 0.169 \left(\frac{2a}{w}\right)^4 \tag{5}$$

and σ is the remote (nominal) stress, defined in Tada et al.[34] as the load over the strip total width.

For the above case b), the expression of K_I is:

$$K_I = 1.122\, g\left(\frac{a}{h}\right) \sigma' \sqrt{\pi a} \tag{6}$$

where g is a polynomial fitting a curve of Tada et al.,[34] p. 264 in the practically relevant range h/a >1.5, see Figures 5 to 16 below:

$$g\left(\frac{a}{h}\right) = 1.000 + 0.127 \left(\frac{a}{h}\right) - 3.190 \left(\frac{a}{h}\right)^2 + 4.958 \left(\frac{a}{h}\right)^3 - 2.503 \left(\frac{a}{h}\right)^4 \tag{7}$$

While the definition of the remote (nominal) stress σ' for the above case b) is unambiguous for the edge-cracked half-plane, when the strip is of finite width it becomes not obvious whether the remote stress should be evaluated as the total load divided by the width of the uncracked portion of the strip, or by the total width. Such uncertainty is resolved in accordance with equation (4) by adopting a σ' value defined as the geometrical mean of the two nominal stress definitions, *i.e.*:

$$\sigma' = \frac{\sigma}{\sqrt{1 - \frac{2a}{w}}} \tag{8}$$

To derive an expression valid for the geometry of Figure 2, various combinations of the two above solutions have been attempted; an accurate and manageable expression was found to be:

$$K_I = 1.122 \frac{\min\left(f\left(\frac{2a}{w}\right), g\left(\frac{a}{h}\right)\right)}{\sqrt{1 - \frac{2a}{w}}} \sigma \sqrt{\pi a} \tag{9}$$

where the *min* function has been introduced to account for the global response being accurately modelled by the disjoint effect of the single, most dominant term, rather than by a joint combination of the two functions *f* and *g*.

An error analysis of formula (9) for K_I has been carried out within the practically relevant ranges $1.5 \leq w/(2a) \leq 40$, $1.5 \leq h/a \leq 50$, employed in Figures 5 to 16 below, and the maximum error has been found to be within ±5 per cent with respect to the FE predictions, see also Appendix 2.

To compactly express the fraction of equation (9), the adimensional term *s* is introduced:

$$s\left(\frac{2a}{w}, \frac{a}{h}\right) = \frac{min\left(f\left(\frac{2a}{w}\right), g\left(\frac{a}{h}\right)\right)}{\sqrt{1 - \frac{2a}{w}}} \tag{10}$$

It is observed that *s* approaches unity for small values of $2a/w$ and a/h.

With the aid of equation (10), the expression of K_I becomes:

$$K_I = 1.122 \; s\left(\frac{2a}{w}, \frac{a}{h}\right) \sigma \sqrt{\pi a} \tag{11}$$

The lead term of the near tip normal stress profile $\hat{p}$ for the cracked strip may be expressed as:

$$\hat{p}(\xi) \approx \frac{K^*}{\sqrt{\xi}} = \frac{K_I}{\sqrt{2\pi\xi}}, \quad \xi << a, h, w \tag{12}$$

where ξ is the distance from the apex, and K^* is a generalized stress intensity factor employed in Sackfield et al.,[8] which is proportional to the classical K_I parameter of the FM field.

It is noted that the above FM expression is independent of the Poisson's ratio, since the so called Michell theorem, see Jeffery,[35] holds, this geometry being simply connected, and the boundary conditions being formulated in terms of stress.

Expression of average stress in terms of seal/strip deformation

As usual, the FM parameter K_I is expressed in equation (11) in terms of the remote tension σ; however, in this application regarding elastomeric seals, a more relevant parameter than the remote tension is the seal fractional compression, κ. Consequently, a FM expression has been developed that is based on the fractional compression imparted to the cracked strip.

By denoting with E^* the equivalent elastic modulus (suitable for describing plane strain conditions), the relation between the fractional compression, κ, and the remote tension, σ, may be expressed as:

$$\sigma = q\left(\frac{2a}{w}, \frac{a}{h}\right)\kappa E^* \tag{13}$$

where the corrective function $q(2a/w, a/h)$ accounts for the fact that in the cracked strip an imposed traction generates unevenly distributed strains as a result of the crack shielding effect, which produces stress-relieved zones in the vicinity of the crack free sides, see Figure 3.

To account for the above discussed uneven strain distribution, a plane version has been developed of a classical approach employed in the design of bolted connections. In this practical approach, a pair of substitutional deformation cone frusta is employed to evaluate the stiffness of the mating members, see the VDI 2230 Standards part I,[36] p. 31. A commonly adopted value for the cone half-angle is $\phi = 30°$. Such substitutional volume represents the tensionally active region of the mating members; its cross sections are supposed to behave in uniaxial stress state according to the elementary theory of a beam subjected to a normal force.

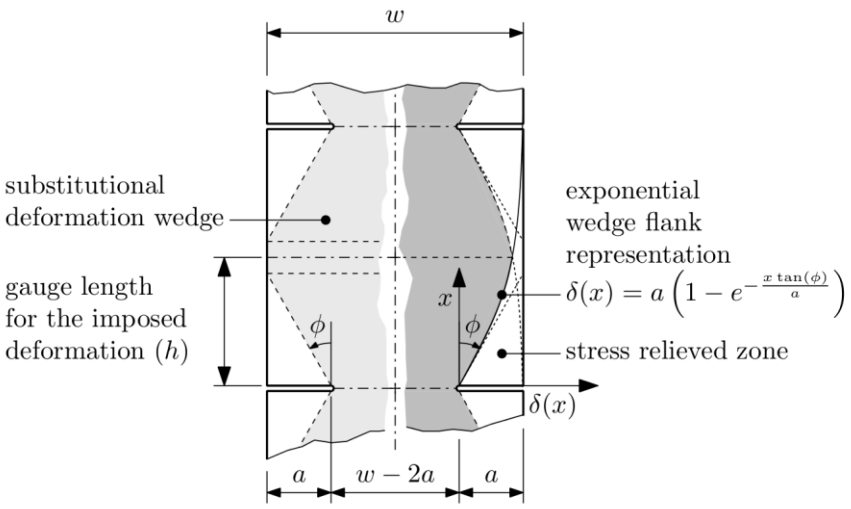

Figure 3. The substitutional plane wedge on the left, and its exponential approximation on the right.

The substitutional double wedge shown in Figure 3 left represents the plane counterpart of the above axisymmetric cone frusta, from which it inherits the assumption of uniaxial, uniform stress along its cross sections; however, a shortcome of this plane model is that two possible situations may occur in which the wedge intersects or otherwise the strip lateral sides. In order to unify the two above possible situations, the exponential description of the active profile shown in Figure 3 right, initially osculating the wedge, and asymptotically approaching the strip sides, has been endorsed in the present paper.

The stiffness corrective factor q of formula (13) is obtained as the ratio between the integral harmonic average of the cross section width of the substitutional profile, and the strip width:

$$q\left(\frac{2a}{w},\frac{a}{h}\right)=\frac{h}{w\int_0^h \frac{1}{w-2a\,e^{-\frac{x}{a}\tan\phi}}dx}=\frac{\tan\phi}{\frac{a}{h}\left[\ln\left(e^{\frac{\tan\phi}{a/h}}-\frac{2a}{w}\right)-\ln\left(1-\frac{2a}{w}\right)\right]} \tag{14}$$

As expected, q approaches unity for small values of $2a/w$ and a/h.

An alternative, more elegant approach suggested by an anonymous reviewer is discussed in Appendix 3.

Asymptotic matching

In this section, an asymptotic matching is carried out between the solution for a semi-infinite rectangular rigid punch with rounded edges indenting a deformable half plane, and for the stress intensity factor of a laterally cracked strip under tension. In particular, by asymptotically matching expressions (3) and (12), the value of d may be formulated as:

$$d=\sqrt[3]{\frac{9\pi^2 r^2 K^{*2}}{4E^{*2}}} \tag{15}$$

By inserting the above value of d into expression (2) for the maximum contact pressure p_{max}, one obtains Formula 21 of Sackfield et al.[8]:

$$p_{max} \cong 1.07 \sqrt[3]{\frac{K^{*2} E^{*}}{r}} \tag{16}$$

Equivalently, it is possible to formulate p_{max} as:

$$p_{max} \cong 0.580 \sqrt[3]{\frac{K_I^{\,2} E^{*}}{r}} = 0.917\ E^{*} \sqrt[3]{\frac{a}{r}\kappa^{2}} \sqrt[3]{q^{2}\left(\frac{2a}{w}, \frac{a}{h}\right) s^{2}\left(\frac{2a}{w}, \frac{a}{h}\right)} \tag{17}$$

where K_I has been expressed by combining equations (11) and (13). In equation (17), p_{max} has been expressed in terms of the equivalent Young's modulus $E^{*} = E/(1-\nu^{2})$, of the ratio a/r, where r is the radius of the rounded edge, and a is the horizontal extent of the protruding material beyond the flat portion of the sealing profile, of the fractional compression, κ, and of the two adimensional factors q, formula (14), and s, formula (10), defined as functions of the two geometrical ratios $2a/w$ and a/h, where w and h are the seal width and height, respectively.

Numerical assessments

Three numerical assessment on the peak contact pressure error incurred by the proposed formulae, with respect to the forecasts of particularly accurate FE models are presented in dedicated sections: the first assessment addresses a specific geometry undergoing an increasing contact extent; the second assessment considers a variety of geometric proportions and compression levels, where, however, the rounded part is described by a quarter circle; the third assessment removes the above restraint by considering rounded parts shorter than a quarter circle, see Figure 1.

Details on the FE model implementations are summarized in Appendix 2.

Numerical assessment of the asymptotically matched formulation when the contact area undergoes a noticeable progression

Before proceeding to an extensive application of the above formulation, it was decided to explore its accuracy when one of the underlying assumptions is gradually weakened, *i.e.* the smallness of the contact width along the rounded portion. In fact in the seal realm the contact width progression may become noticeable with respect to the seal characteristic dimensions. A reference rectangular seal is considered that is defined by the following normalized geometrical parameters and elastic constants: $w/r = 3.78$, $h/r = 3.33$, $r/a = 2$, $E \approx 3.52$ MPa, $\upsilon = 0.489$, see Strozzi,[4] Strozzi et al.,[7] and Prati and Strozzi.[11]

The fractional compression, which is normally a design parameter, is here treated as a dependent variable; in fact, a semi-inverse approach has been adopted in the FE forecasts, in order to limit the nonlinearities to that induced by the progressive nature of the contact.

The FE model is shown in the inset of Figure 4 , and it considers the actual problem of an elastic body whose profile is partially flat and partially circular, pressed against a rigid flat counter plane, see Figures 1 and 2a.

The above case, named (a), differs from the idealized geometry (b) treated in Sackfield et al.,[8] in three distinct aspects: i) in (a) the body is of finite dimension whereas in (b) it is infinite; ii) in (a) the elastic body is profiled, and the rigid counterplane is flat, whereas in (b) the elastic body is flat, and the rigid counterpart is profiled; iii) in (a) a circular profile is adopted, whereas in (b) a parabolic approximation is used.

The main aim of this section is to evaluate the level of accuracy that a design formula for the peak pressure based on equation (16) may reach; consequently, only the cumulative error induced by the three mentioned discrepancies is here reported.

In evaluating the peak contact pressure according to equation (16), the particularly accurate numerical coefficient 1.07335 has been used within the contest of the error analysis of Figure 4; in addition, the generalized stress intensity factor K^* has been evaluated with a dedicated FE analysis tailored on the above reference seal

geometry, and based upon the approach of Smith and Della-Ventura.[37] This dedicated analysis has been adopted in compiling Figure 4 to avoid the errors incurred by the employment of a stress intensity factor based on the *s*, *q* estimates, see formula (17).

Figure 4 illustrates the relative error ε

$$\varepsilon = \frac{p_{\max,\ eq\ 16}}{p_{\max,\ FE}} - 1 \qquad (20)$$

on the peak pressure, incurred by equation (16) with respect to the FE modelling.

The error curve is plotted versus the ratio between the contact extent along the rounded region, *d*, and the shortest amongst the elastic substrate characteristic dimensions, namely the seal section height, *h*, the half width of the flat portion of the sealing profile, (*w/2*-*a*), and the protrusion extent, *a*; in the reference geometry, the latter, *a*, is the most restraining dimension, so that the above ratio is *d/a*.

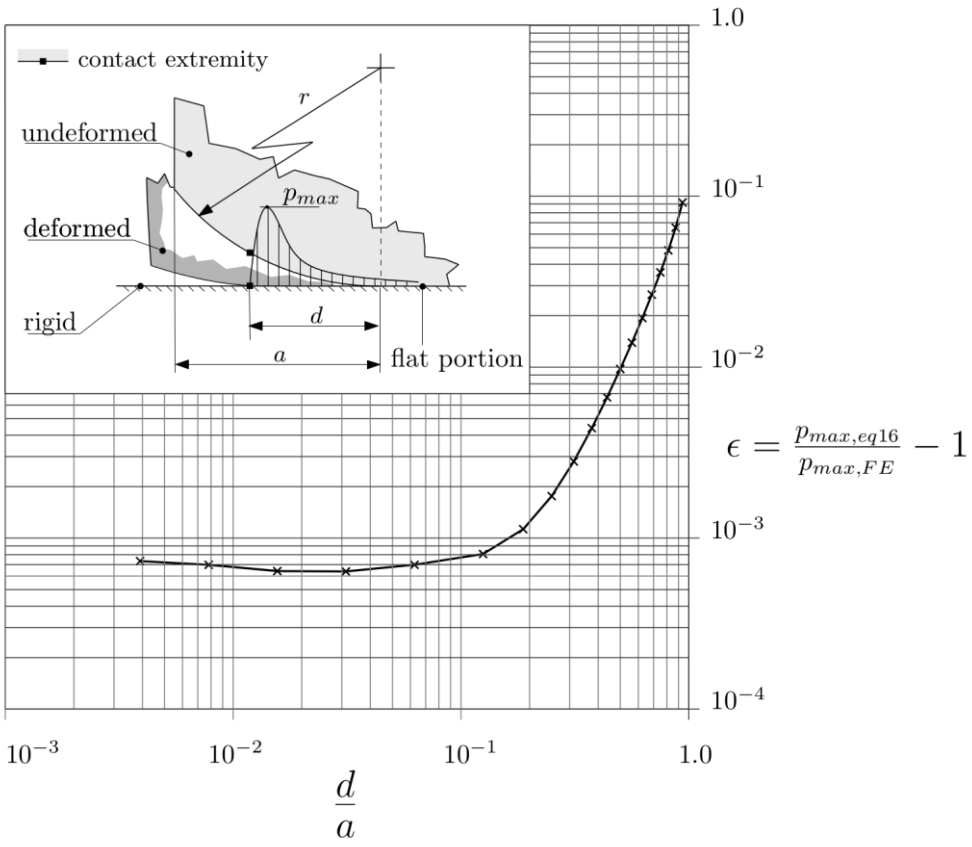

Figure 4. Comparison between the relative error on the peak contact pressure according to formula (20) incurred by the analytical approach with respect to the FE forecasts.

Figure 4 shows that the error remains lower than 1 per cent when the contact extent of the rounded portion is smaller than about half the protrusion extent, *i.e.* d/a = 1/2. This result gets confidence in the employment of this approach for applications in the seal realm. The validity of this result is limited to the contacting profile here examined; its extension to different profiles would require further investigations.

Numerical assessment of the analytical expression of the contact pressure peak for a rounded edge shaped as a quarter of circumference

As already mentioned, the asymptotically corrected analytical expression (17) of the peak contact pressure should account for four dimensional geometrical parameters, namely: i) the extent of the projection of the lateral parts beyond the flat portion of the sealing profile, a; ii) the seal width, w; iii) the seal height, h; iv) the rounding radius, r. Consequently, the normalized parameters describing the seal geometry are three. In this Section, only a rounded edge described by a quarter of circumference is considered; for this geometry, a equals r. Consequently, the normalized geometrical parameters considered in this Section are two, namely $w/(2r)$ and h/r, to which the value must be added of the fractional compression, κ, imparted to the seal.

It is too difficult to derive analytically an error estimate of formula (17), detailed information on the pressure peak values for a spectrum of seal geometries being unavailable. It was therefore decided to carry out an error analysis on formula (17) with the aid of FE.

In order to focus on the ability of the asymptotically corrected analytical expression (17) to account for the three above normalized parameters in predicting the contact pressure peaks, it was decided to adopt for the time being linear elasticity, and to postpone the exploration of large deformation effects to a dedicated section.

Four error diagrams, Figures 5 to 8, reporting $w/(2r)$ along the x-axis, and h/r along the y-axis, have been compiled; the x-variable $w/(2r)$ ranges between 1.5 and 40; the y-variable h/r ranges between 1.5 and 50; such intervals generously encompass practically relevant geometries of rectangular seals, see the literature review. The four diagrams refer to fractional compressions, κ, of 1, 5, 10, 15 per cent, respectively; the contour lines define the relative error between the pressure peak obtained with the asymptotic formula (17), and with FE, assumed as the reference value; a positive error means that the asymptotic formula overrates the FE predictions.

The error generally increases with the fractional compression, and this trend is imputable to the weakening of the assumption related to a small contact extent along the rounded profile, as it emerges from Figure 4.

The most interesting zone of the diagrams is the upper-right corner, since it covers most of the technically relevant seal shapes. In this zone, the relative error is lower than the fractional compression imparted.

Formula (17) becomes less accurate in the vicinity of the lower-left corner of the diagrams, that is, for relatively low values of $w/(2r)$ and h/r, a condition, this, in which the two lateral pressure peaks may interact. In this diagram corner, the flat portion of the sealing profile becomes very small, and, therefore, the seal section approaches a portion of an O-ring described by a circular segment. In Figure 2 of Ciavarella et al.,[6] it is shown that the analytical pressure profile becomes Hertzian for low values of the flat

portion of the sealing profile. For such seal geometries, a direct application of the formulas available for O-ring seals, George et al.,[2] is perhaps preferable.

As a final remark, the asymptotic expression (19) derived in Strozzi et al.[7] for the peak contact pressure, was found to be independent of the rounding radius, whereas in diagrams 5 to 8 the rounding radius plays a relevant role, especially when it is relatively large. This apparent contradiction may be resolved by observing that formula (19) of Strozzi et al.,[7] addresses an infinitely wide and high seal, whereas in Figures 5 to 8 the effect of the seal finite dimensions is accounted for, albeit approximately. The limited error gradients observed in the proximity of the upper-right corner of the diagrams confirm the fact that the influence of the rounding radius becomes progressively small for large values of *w* and *h*.

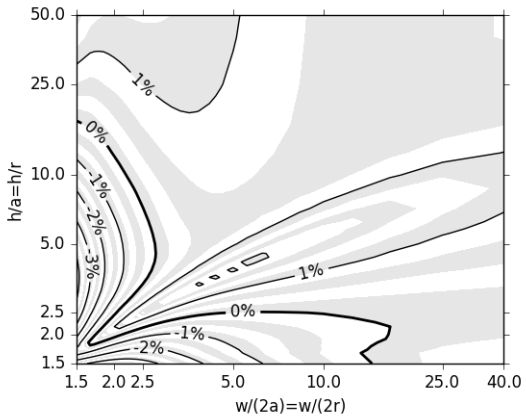

Figure 5. Relative error on the peak contact pressure according to formula (17) with respect to FE forecasts for a fractional compression κ of 1 per cent.

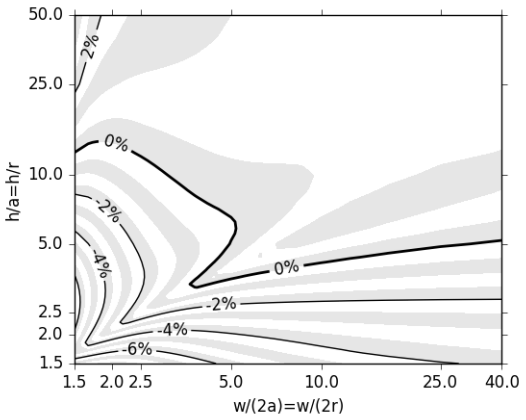

Figure 6. Relative error on the peak contact pressure according to formula (17) with respect to FE forecasts for a fractional compression κ of 5 per cent.

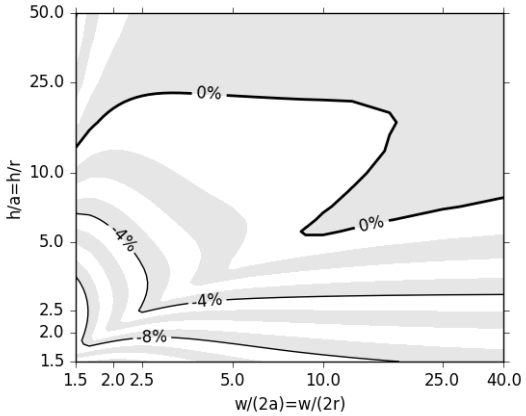

Figure 7. Relative error on the peak contact pressure according to formula (17) with respect to FE forecasts for a fractional compression κ of 10 per cent.

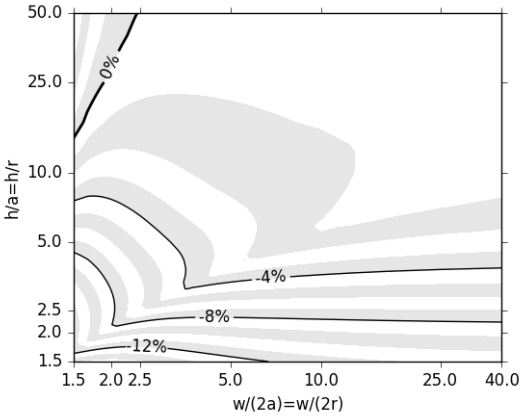

Figure 8. Relative error on the peak contact pressure according to formula (17) with respect to FE forecasts for a fractional compression κ of 15 per cent.

As an example of the application of the previous formulae, a rectangular elastomeric seal is considered that is defined by the following dimensions and elastic constants, extracted from Stupkiewicz and Marciniszyn[18]: width w = 3.5 mm, height h = 5.15, edge radius r = 0.1, 0.2, 0.4 mm, fractional compression, κ = 2.91 per cent, $E \approx 3G$ = 10.98 MPa (the Poisson's ratio adopted in Stupkiewicz and Marciniszyn[18] is υ = 0.496; the relevance of υ has been discussed in the literature review).

For the three edge radii r = 0.1, 0.2, 0.4 mm, the maximum peak contact pressure forecast by formula (17) is 1.262, 1.257, 1.237, respectively, whereas its counterpart derived from FE is 1.252, 1.246, 1.227 MPa, respectively; for all three cases, the relative error is lower than 1 per cent, and it is consistent with Figures 5 and 6, dealing

with fractional compressions of 1 and 5 per cent, respectively, encompassing the κ = 2.91 value.

Numerical assessment of the analytical expression of the contact pressure peak for a rounded border shorter than a quarter circumference

In this Section, seal geometries are addressed in which the extent of the rounded border is shorter than a quarter circumference, see Figure 1. To limit the number of independent variables, only geometries described by $r/a = 2$, see Strozzi,[4] and Prati and Strozzi,[11] are considered in this study.

Four error diagrams 9 to 12 have been compiled that are analogous to Figures 5 to 8; these diagrams report w/r along the x-axis, and $2h/r$ along the y-axis for geometries defined by $a = r/2$; they refer to fractional compressions, κ, of 1, 5, 10, 15 per cent, respectively; the contour lines define the relative error between the pressure peak obtained with the asymptotic formula (17), and with FE, the latter being assumed as reference.

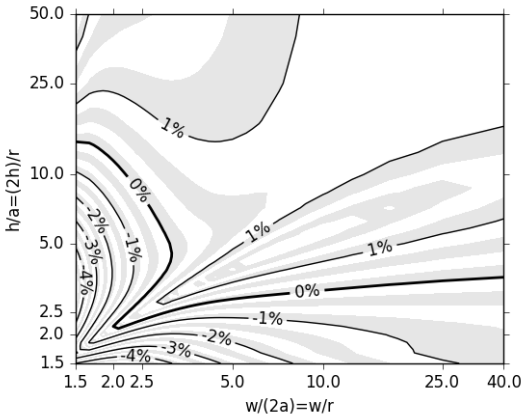

Figure 9. Relative error on the peak contact pressure according to formula (17) with respect to FE forecasts for $a = r/2$ and for a fractional compression κ of 1 per cent.

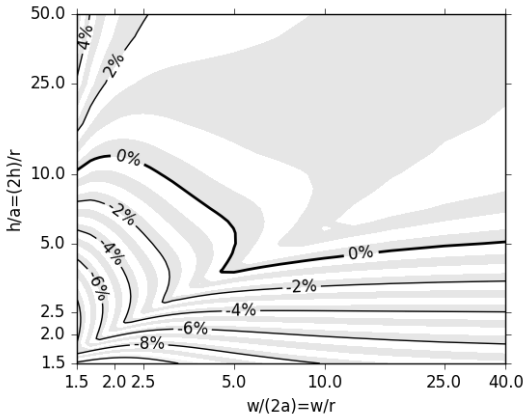

Figure 10. Relative error on the peak contact pressure according to formula (17) with respect to FE forecasts for $a = r/2$ and for a fractional compression κ of 5 per cent.

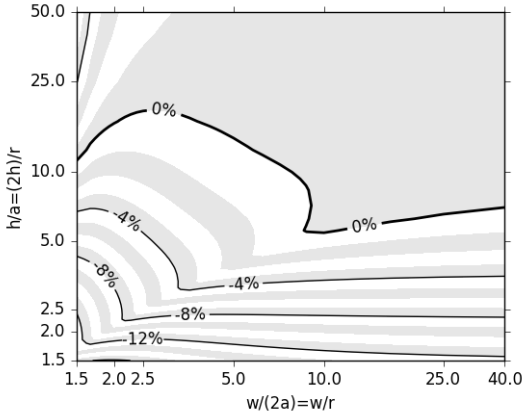

Figure 11. Relative error on the peak contact pressure according to formula (17) with respect to FE forecasts for $a = r/2$ and for a fractional compression κ of 10 per cent.

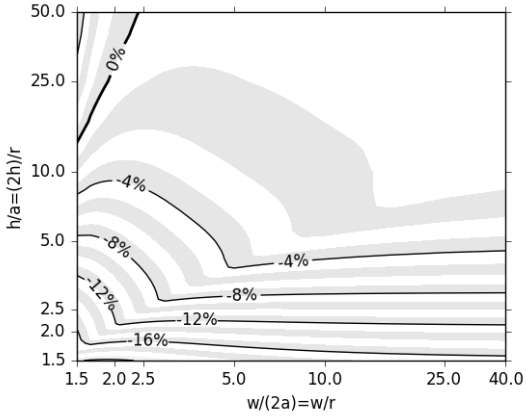

Figure 12. Relative error on the peak contact pressure according to formula (17) with respect to FE forecasts for $a = r/2$ and for a fractional compression κ of 15 per cent.

The fractional compressions examined have been confined to 15 per cent, since for moderately higher compressions the contact length may extend to the whole sealing profile, see Strozzi;[4] in this case, the contact pressure no longer vanishes at the contact extremities, and formula (17) becomes inapplicable.

Numerical assessment of the error incurred by large deformations

In this Section, the effect of large deformations is explored with FE, and the numerical forecasts are compared to a modified version of the design formula (17).

To confine this error analysis to the effect of large deformations, thus essentially disregarding the influence of the constitutive relationship, in the FE study of this section the compressible neo-Hookean constitutive relationship has been adopted, since it constitutes the natural extension to large deformations of the Hooke law employed in small deformations. The material constants of the neo-Hookean constitutive relationship are derived from the Young's modulus and the Poisson ratio used in the small deformation theory.

The analytical formulas have been modified by adopting a definition of the seal compression ratio κ' suitable for large strains, *i.e.*

$$\kappa' = \frac{\kappa h}{h - \kappa h} = \frac{\kappa}{1 - \kappa} \tag{21}$$

where κh is the seal height reduction, see Figure 2. It is noted that in this definition the reference length (h-κh) is expressed with regard to the deformed configuration.

By substituting κ with κ' in equations (13) and (17), corrected mean and peak contact pressure values are obtained.

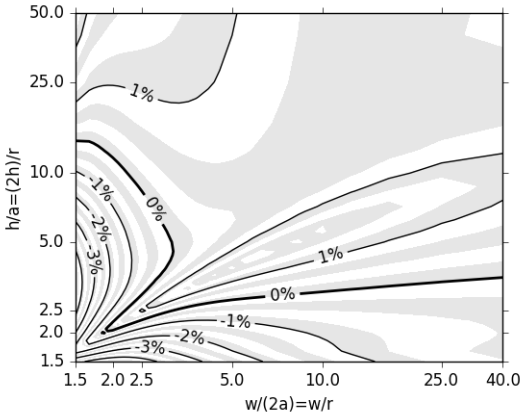

Figure 13. Relative error on the peak contact pressure according to formula (17) with respect to FE forecasts for $a = r/2$ and for a fractional compression κ of 1 per cent.

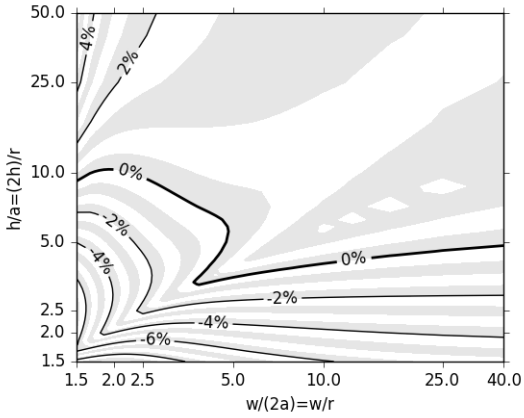

Figure 14. Relative error on the peak contact pressure according to formula (17) with respect to FE forecasts for $a = r/2$ and for a fractional compression κ of 5 per cent.

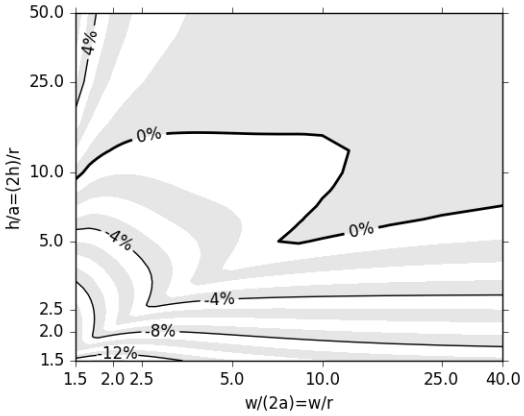

Figure 15. Relative error on the peak contact pressure according to formula (17) with respect to FE forecasts for $a = r/2$ and for a fractional compression κ of 10 per cent.

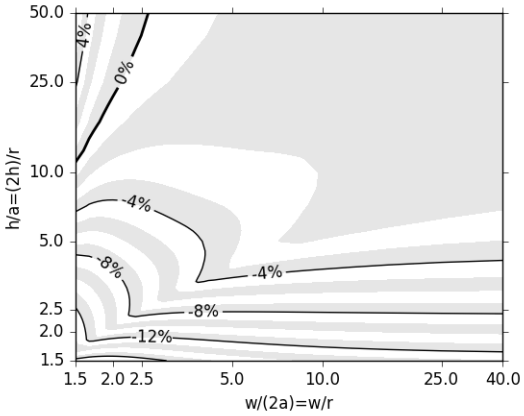

Figure 16. Relative error on the peak contact pressure according to formula (17) with respect to FE forecasts for $a = r/2$ and for a fractional compression κ of 15 per cent.

Four error diagrams, Figures 13 to 16, have been compiled that are analogous to diagrams 9 to 12; these diagram report w/r along the x-axis, and $2h/r$ along the y-axis for geometries defined by $a = r/2$; for consistency with Figures 9 to 12, they refer to the small strain definition of the fractional compression, κ, of 1, 5, 10, 15 per cent, respectively; the contour lines define the relative error between the pressure peak obtained with the corrected asymptotic formula (17), in which κ' is used instead of κ, versus FE forecasts; consistent with the large strain assumption, the Cauchy definition of contact normal stress is now employed in the FE predictions.

Surprisingly, the errors are similar to their counterparts incurred in linear elasticity.

As an example of the application of the previous formulae, the rectangular elastomeric seal is considered that has already been examined in section "*Numerical assessment of the asymptotically matched formulation when the contact area undergoes a noticeable progression*". The seal is defined by the following normalized geometrical parameters and elastic constants: $w/r = 3.78$, $h/r = 3.33$, $r/a = 2$, $E \approx 3.52$ MPa, $\upsilon = 0.489$, and by a fractional compression $\kappa = 15$ per cent, see Strozzi,[4] Strozzi et al.,[7] and Prati and Strozzi.[11] The maximum peak contact pressure forecast by the corrected formula (17) is 1.011 MPa. Moving to the FE peak pressure, its value is 1.031 MPa under large strain assumptions, it is 0.941 MPa under small strain assumptions, whereas the finite elasticity value reported in Strozzi[4] is 1.05 MPa. This example confirms the practical usefulness of the proposed methodology.

Conclusions

The contact pressure in an elastomeric rectangular seal with rounded edges has been considered. An asymptotic matching has been performed between an available analytical expression of the contact pressure that neglects the finiteness of the seal dimensions, and a fracture mechanics solution describing a periodically, laterally cracked strip of finite width. This matching has provided a corrected formula for the peak contact pressure that accounts for the finiteness of the seal dimensions. An extensive error analysis of the proposed formula has been performed with the aid of

Finite Elements. The analytical expression for the peak contact pressure has been validated versus numerical predictions for a large family of seal geometries and, in particular, for a seal reference shape extracted from the pertinent literature. Finally, an appraisal of the finite deformation effect has been carried out numerically. The error has been found to be technically acceptable for practically relevant seal geometries.

Declaration of conflicting interests

The authors declare that there is no conflict of interest.

Funding

This research received no specific grant from any funding agency in the public, commercial, or not-for-profit sectors.

References

1. Nikas GK, Almond RV and Burridge G. Experimental Study of Leakage and Friction of Rectangular, Elastomeric, Hydraulic Seals for Reciprocating Motion from− 54 to+ 135° C and Pressures from 3.4 to 34.5 MPa. *Tribol Trans* 2014; 57(5): 846–865.
2. George AF, Strozzi A and Rich JI. Stress fields in a compressed unconstrained elastomeric O-ring seal and a comparison of computer predictions and experimental results. *Tribol Int* 1987; 20(5): 237–247.

3. Ruskell LEC. A rapidly converging theoretical solution of the elastohydrodynamic problem for rectangular rubber seals. *J Mech Eng Sci* 1980; 22(1): 9–16.

4. Strozzi A. Static stresses in an unpressurized, rounded, rectangular, elastomeric seal. *ASLE Trans* 1986; 29(4): 558–564.

5. Strozzi A, Baldini A, Giacopini M, et al. Normalization of the stress concentrations at the rounded edges of a shaft–hub interference fit. *J Strain Anal* 2011; 46(6): 478–491.

6. Ciavarella M, Hills DA and Monno G. The influence of rounded edges on indentation by a flat punch. *Proc Inst Mech Engs, Part C: J Mech Eng Sci* 1998; 212(4): 319–328.

7. Strozzi A, Bertocchi E, Baldini A, et al. On the applicability of the Boussinesq influence function in modelling the frictionless elastic contact between a rectangular indenter with rounded edges and a half-plane. *Proc Inst Mech Engs, Part C: J Mech Eng Sci* 2014; 0954406214542641.

8. Sackfield A, Mugadu A, Barber JR, et al. The application of asymptotic solutions to characterising the process zone in almost complete frictionless contacts. *J Mech and Phys of Solids* 2003; 51(7): 1333–1346.

9. Banerjee N, Hills DA and Dini D. The derivation and application of a semi-infinite flat and rounded asymptotic frictionless contact. *Int J Mech Sci* 2009; 51: 662–666.

10. Prati E and Strozzi A. A study of the elastohydrodynamic problem in rectangular elastomeric seals. *J Tribol* 1984; 106(4): 505–512.

11. Nikas GK. Elastohydrodynamics and Mechanics of Rectangular Elastomeric Seals for Reciprocating Piston Rods. *ASME J Tribol* 2003; 125(1): 60–69.

12. Nikas GK. Analytical study of the extrusion of rectangular elastomeric seals for linear hydraulic actuators. *Proc Inst Mech Eng, Part J: J Eng Tribol* 2003;217(5): 365–373.

13. Nikas GK. Transient elastohydrodynamic lubrication of rectangular elastomeric seals for linear hydraulic actuators. *Proc Inst Mech Eng, Part J: J Eng Tribol* 2003; 217(6): 461–473.

14. Nikas GK and Sayles RS. Nonlinear elasticity of rectangular elastomeric seals and its effect on elastohydrodynamic numerical analysis. *Tribol Int* 2004; 37(8): 651–660.

15. Nikas GK and Sayles RS. Modelling and optimization of composite rectangular reciprocating seals. *Proc Inst Mech Eng, Part J: J Eng Tribol* 2006; 220(4): 395–412.

16. Nikas GK and Sayles RS. Study of leakage and friction of flexible seals for steady motion via a numerical approximation method. *Tribol Int* 2006; 39(9): 921–936.

17. Nikas GK and Sayles RS. Computational model of tandem rectangular elastomeric seals for reciprocating motion. *Tribol Int,* 2006; 39(7): 622–634.

18. Stupkiewicz S and Marciniszyn A. Elastohydrodynamic lubrication and finite configuration changes in reciprocating elastomeric seals. *Tribol Int* 2009; 42(5): 615–627.

19. Medri G and Strozzi A. Mechanical analysis of elastomeric seals by numerical methods. *Industrial & Eng Chemistry Product Research and Development* 1984; 23(4): 596–600.

20. Rana A, Sayles R, Nikas GK, et al. An experimental technique for investigating the sealing principles of reciprocating elastomeric seals for use in linear hydraulic actuator assemblies. In: *Proc. of 2nd World Tribol Congress,* Vienna, Austria 2001.

21. Dowson D and Swales PD. The development of elastohydrodynamic conditions in a reciprocating seal. In: *Proc. 4th Int. Conf. on Fluid Sealing* 1969; 2: 2–10.

22. Field GJ and Nau BS. An experimental study of reciprocating rubber seals. In: *Proc. Instns Mech. Engrs, Symposium on Elastohydrodynamic Lubrication* 1972; 29–36.

23. Field GJ and Nau BS. Film thickness and friction measurements during reciprocation of a rectangular section rubber seal ring. In: *Proc. of the sixth BHRA Int. conference on fluid sealing* 1973; 5: 45–56.

24. Field GJ and Nau BS. A theoretical study of the elastohydrodynamic lubrication of reciprocating rubber seals. *ASLE Trans* 1975; 18(1): 48–54 (1975).

25. Lindley PB. Compression characteristics of laterally–unrestrained rubber O-rings. *J. Inst. Rubber Ind*, 1967; 1(4): 209–213.

26. Stupnicki J. Photoelastic Study of the Influence of Oil Film on Contact Stresses. *Int. J Mech Sci*, 1971; 13(3): 243–250.

27. Dragoni E and Strozzi A. Theoretical analysis of an unpressurized elastomeric O-ring seal inserted into a rectangular groove. *Wear* 1989; 130(1): 41–51.

28. Strozzi A and Unsworth A. An Appraisal of the Paper by O'Carrol et al.(1990). *Proc Inst Mech Eng, Part H: J Eng Medicine* 1995; 209(3): 203–205.

29. Lindley PB. *Engineering design with natural rubber*. Natural Rubber Producers' Research Ass, 1970.

30. Allen PW, Lindley PB and Payne AR. *Use of Rubber in Engineering* London: Maclaren and Sons Ltd, 1976.

31. Strozzi A. *Contact stresses in hip replacements*. PhD Thesis, University of Durham, UK, 1992.

32. Holownia BP. Effect of Poisson's ratio on bonded rubber blocks. *J Strain Anal*, 1972; 7(3): 236–242.

33. Medri G and Strozzi A. Stress-strain fields in compressed elastomeric seals and their extension to fracture mechanics. *Rubber Chemistry and Technology*, 1986; 59(5): 709–721.

34. Tada H, Paris PC and Irwin GR. The stress analysis of cracks handbook ASME. *New York*, 55–56 (2000).

35. Jeffery GB. Plane stress and plane strain in bipolar co-ordinates. *P Roy Soc Lond Series A* 1921; 221: 265–293.

36. VDI 2230 part 1 – Systematic calculation of high duty bolted joints, Joints with one cylindrical bolt. VDI Richtlinien, 31 (2003).

37. Smith RNL and Della-Ventura D. A superposition method for the solution of crack problems. *Communications in numerical methods in engineering* 1995; 11(3): 243–254.

38. Johnson KL. One hundred years of Hertz contact. *Proc Inst Mech Eng*s 1982; 196(1): 363–378.

39. Olukoko OA, Becker AA and Fenner RT. Three benchmark examples for frictional contact modelling using finite element and boundary element methods. *J Strain Anal* 1993; 28; 293–301.

Appendix 1: list of symbols

a	extent of the rounded portion of the seal (or crack extent)
d	extent of the contact along the seal rounded portion
E	Young's modulus
E^*	equivalent Young's modulus
f	auxiliary function
g	auxiliary function

h	seal height (or edge crack half-period)
K^*	generalized stress intensity factor
K_I	stress intensity factor
p	contact pressure
$\hat{p}$	lead term of the normal stress profile in the cracked strip
p_{max}	maximum contact pressure
q	stiffness corrective function
r	seal corner radius
s	auxiliary function
w	seal width (or strip width)
δ	function describing the wedge side
κ	seal fractional compression for small strains
κ'	alternative definition of seal fractional compression for large strains
ν	Poisson's ratio
ξ	local coordinate along the contact length
σ	remote tension
σ'	alternative definition of remote tension
ϕ	substitutional cone half-angle

Appendix 2

Details on the FE modeling are given below. The commercial solver MSC.Marc 2013 has been employed in all simulations. Particular attention has been paid to the discretization of the rounded zone, since, following Olukoko et al.,[39] at least 10 nodes should define the progressive extent of the contact zone.

Three different kinds of FE models have been used, depending on specific implementation requirements.

The FE campaign referred to in the section "*FM expression derived from existing solutions"* aims at evaluating the stress intensity factor K_I for the cracked strip geometry of Figure 2b under an imposed elongation. This FE prediction has been used to assess the accuracy of Formula (9). A family of 155 models spans the domain. The J-integral approach implemented in the MSC.Marc solver has been used. The near tip region is modelled with 8 noded isoparametric elements, whereas the remaining domain is dynamically meshed with 6 noded isoparametric triangular elements. The ratio between the element size at the tip and the smallest characteristic strip dimension is kept lower than 1/30. A twice finer mesh has been used to assess convergence.

The FE models referred to in the section "*Numerical assessment of the asymptotically matched formulation when the contact area undergoes a noticeable progression*" use a graded mesh consisting of 94530 eight-noded isoparametric elements, with 4096 elements along the rounded portion of the sealing profile, and it is

gradually coarsened when departing from the aforementioned contact region. The progressive contact is treated according to the semi-inverse approach, which combines the results of two linear analyses, whose contact extent is imposed and equal. The number of nodes in contact beyond the flat portion of the sealing profile grows from 16 to some thousands depending on the imposed contact extent. The same mesh was used with appropriate boundary conditions in evaluating the K^* stress singularity factor according to the Smith and Della-Ventura[37] method. The reference mesh is built by adopting the parabolic geometry of the inset of Figure 4; in the K^* FE evaluation, a flattened variant of the same mesh has been obtained by morphing.

The FE forecasts used as reference in compiling the error maps of Figures 5 to 16 are based on a family of 1261 models, detailed as follows. The mesh locally describing the rounded portion of the profile has been kept unvaried, and it consists of about 12000 (20000) four noded isoparametric elements in the case $r=2a$ ($r=a$), with a local element size equal to $a/300$, which gradually coarsens departing from the progressive contact region. The remaining elastic domain has been dynamically meshed according to the specific extents of the geometry, with a gradual coarsening. The peak contact pressure has been evaluated with no less than 24 contacting nodes along the rounded portion. The nonlinear node to segment contact algorithm of the MSC.Marc solver has been employed in modelling the progressive contact; the use of bilinear (as

opposed to biquadratic, see above) elements coupled with the specific contact routines is recommended in the MSC.Marc manual.

Appendix 3

An alternative, more elegant approach for defining the stiffness corrective factor q has been suggested by an anonymous reviewer, that is based on the Betti theorem and on an estimate of the crack opening displacement (COD), e.g., the classical square root COD function quoted in Tada et al.,[34] in terms of its integral value.

By adopting the K_I of equation (11) to scale such COD function, the resulting expression for the q function is

$$q\left(\frac{2a}{w},\frac{a}{h}\right)=\frac{1}{1+\frac{4\sqrt{2}}{3}\frac{2a}{w}\frac{a}{h}1.122\,s\left(\frac{2a}{w},\frac{a}{h}\right)} \tag{22}$$

Unfortunately, the assumed COD loses its accuracy as the distance from the crack tip becomes comparable to the problem characteristic dimensions, *e.g.*, the crack length a; for example, in the geometry characterized by the ratios $w/r = 3.78$, $h/r = 3.33$, $r/a = 2$, see Strozzi,[4] the error on the integral of the assumed COD with respect to a dedicated FE analysis is about 7 per cent, which results in a relative error on the average pressure of about 6.5 per cent, whereas the error of the substitutional wedge approach is 0.9 per cent.

An error analysis carried out on the intervals of Figures 5 to 8 showed that the two methods produce comparable cumulative errors in terms of peak pressure; it was decided to present here only the substitutional wedge approach.